



**Providing Choice & Value**  
Generic CT and MRI Contrast Agents

**FRESENIUS  
KABI**

**CONTACT REP**

**AJNR**

## **Is Contrast Medium Really Needed for Follow-up MRI of Untreated Intracranial Meningiomas?**

J. Boto, R. Guatta, A. Fitsiori, J. Hofmeister, T.R. Meling and M.I. Vargas

This information is current as of July 29, 2025.

*AJNR Am J Neuroradiol* 2021, 42 (8) 1421-1428

doi: <https://doi.org/10.3174/ajnr.A7170>

<http://www.ajnr.org/content/42/8/1421>

# Is Contrast Medium Really Needed for Follow-up MRI of Untreated Intracranial Meningiomas?

J. Boto, R. Guatta, A. Fitsiori, J. Hofmeister, T.R. Meling, and M.I. Vargas



## ABSTRACT

**BACKGROUND AND PURPOSE:** Recent concerns relating to tissue deposition of gadolinium are favoring the use of noncontrast MR imaging whenever possible. The purpose of this study was to assess the necessity of gadolinium contrast for follow-up MR imaging of untreated intracranial meningiomas.

**MATERIALS AND METHODS:** One-hundred twenty-two patients (35 men, 87 women) with meningiomas who underwent brain MR imaging between May 2007 and May 2019 in our institution were included in this retrospective cohort study. We analyzed 132 meningiomas: 73 non-skull base (55%) versus 59 skull base (45%), 93 symptomatic (70%) versus 39 asymptomatic (30%). Fifty-nine meningiomas underwent an operation: 54 World Health Organization grade I (92%) and 5 World Health Organization grade II (8%). All meningiomas were segmented on T1 3D-gadolinium and 2D-T2WI. Agreement between T1 3D-gadolinium and 2D-T2WI segmentations was assessed by the intraclass correlation coefficient.

**RESULTS:** The mean time between MR images was 1485 days (range, 760–3810 days). There was excellent agreement between T1 3D-gadolinium and T2WI segmentations ( $P < .001$ ): mean tumor volume (T1 3D-gadolinium: 9012.15 [SD, 19,223.03] mm<sup>3</sup>; T2WI: 8528.45 [SD, 18,368.18] mm<sup>3</sup>; intraclass correlation coefficient = 0.996), surface area (intraclass correlation coefficient = 0.989), surface/volume ratio (intraclass correlation coefficient = 0.924), maximum 3D diameter (intraclass correlation coefficient = 0.986), maximum 2D diameter in the axial (intraclass correlation coefficient = 0.990), coronal (intraclass correlation coefficient = 0.982), and sagittal planes (intraclass correlation coefficient = 0.985), major axis length (intraclass correlation coefficient = 0.989), minor axis length (intraclass correlation coefficient = 0.992), and least axis length (intraclass correlation coefficient = 0.988). Tumor growth also showed good agreement ( $P < .001$ ), estimated as a mean of 461.87 [SD, 2704.1] mm<sup>3</sup>/year on T1 3D-gadolinium and 556.64 [SD, 2624.02] mm<sup>3</sup>/year on T2WI.

**CONCLUSIONS:** Our results show excellent agreement between the size and growth of meningiomas derived from T1 3D-gadolinium and 2D-T2WI, suggesting that the use of noncontrast MR imaging may be appropriate for the follow-up of untreated meningiomas, which would be cost-effective and avert risks associated with contrast media.

**ABBREVIATIONS:** Gd = gadolinium; ICC = intraclass correlation coefficient; WHO = World Health Organization

Recent concerns regarding gadolinium (Gd) compounds are fueling a trend to use contrast media in MR imaging less frequently. Notwithstanding the well-established safety profile of Gd compounds, a small number of immediate adverse effects, which may be life-threatening, has been reported<sup>1,2</sup> at a rate of

approximately 0.3%.<sup>2</sup> Furthermore, repeat administration of Gd-based contrast may lead to deposition of Gd in the dentate nucleus and the globus pallidus,<sup>3–7</sup> which seems to be the case with linear rather than macrocyclic Gd compounds,<sup>4</sup> despite a normal renal function<sup>7</sup> and an intact blood-brain barrier.<sup>6</sup> Health care costs should also be considered because they are a heavy burden to modern Western societies,<sup>8–10</sup> and medical imaging accounts for a large proportion of these costs.<sup>10</sup> Gd-based contrast media significantly contribute to the cost of an MR image, due to the price of the contrast medium itself and also because of the prolonged image-acquisition time. Using contrast media more sparingly could, therefore, reduce these costs considerably.

The above-mentioned concerns are particularly pertinent to young patients with incidental or asymptomatic meningiomas in which frequent and long-term follow-up MR imaging is usually

Received September 17, 2020; accepted after revision March 8, 2021.

From the Divisions of Neuroradiology (J.B., A.F., J.H., M.I.V.) and Neurosurgery (T.R.M.), Geneva University Hospital and Faculty of Medicine of Geneva, Geneva, Switzerland; and Division of Neurosurgery (R.G.), Lugano Regional Hospital (Civic), Lugano, Switzerland.

Please address correspondence to José Boto, MD, MSc, Geneva University Hospitals, Division of Neuroradiology, Rue Gabrielle-Perret-Gentil 4, 1205 Genève, Switzerland; e-mail: jose.m.baiaoboto@hcuge.ch



Indicates article with online supplemental data.

<http://dx.doi.org/10.3174/ajnr.A7170>

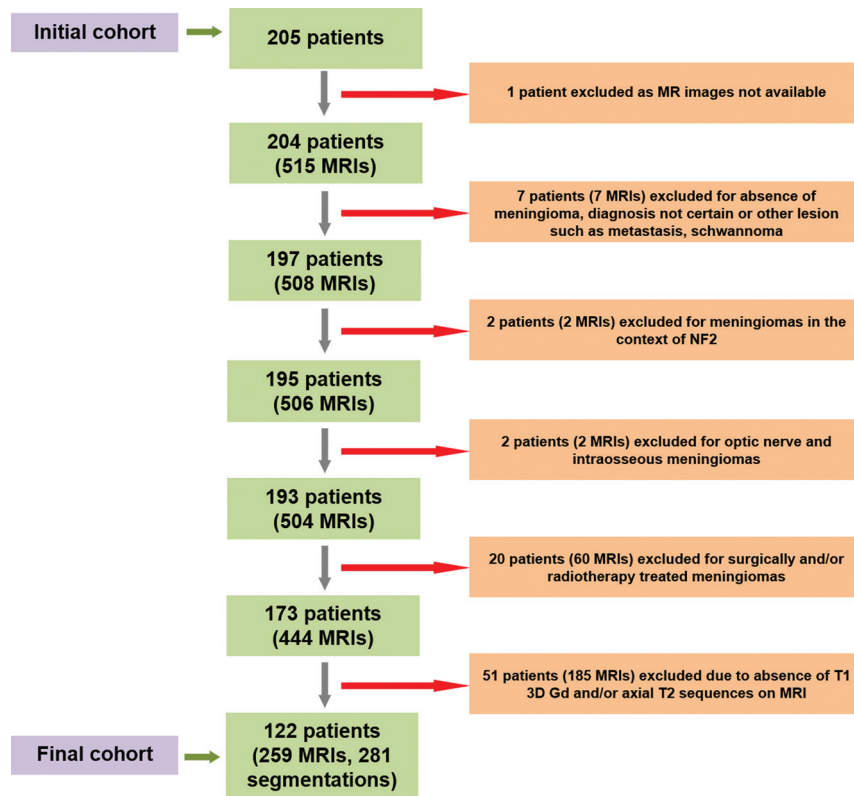


**FIG 1.** Flow diagram showing the steps in patient selection. NF2 indicates neurofibromatosis type 2.

performed, the current standard-of-care being MR with Gd-based contrast media.<sup>11</sup> Intracranial meningiomas are, by and large, benign World Health Organization (WHO) grade I tumors derived from meningotheelial cells,<sup>12,13</sup> representing approximately one-third of all primary central nervous system tumors<sup>14</sup> and 15% of symptomatic intracranial masses.<sup>15</sup> They are extra-axial lesions that usually exhibit slow growth (approximately 14%/year for WHO grade I lesions).<sup>16</sup> However, the growth rate can be substantially higher, particularly in WHO grade II and III meningiomas, necessitating frequent MR imaging follow-up. For instance, the European Association of Neuro-Oncology advocates diligent radiologic follow-up of meningiomas. For small asymptomatic meningiomas, the recommendation of this institution is to assess the tumor dynamics with contrast MR imaging at 6 months after the initial diagnosis and then annually as long as the patient remains asymptomatic.<sup>11</sup>

Quantitative MR imaging parameters such as tumor volume<sup>17</sup> are important in predicting tumor growth and behavior. Nakasu and Nakasu,<sup>18</sup> in 2020, identified large tumor size and annual volume change of  $\geq 2.1 \text{ cm}^3$  as the strongest predictors of symptomatic tumor progression. Several other parameters may be important in predicting the potential for rapid tumor growth, such as male sex,<sup>18</sup> younger age,<sup>18</sup> absence of calcification,<sup>18-23</sup> peritumoral edema,<sup>21,22,24</sup> and hyperintensity on T2WI.<sup>18,19,22,25,26</sup>

Considering these points, the purpose of this retrospective cohort study was to assess the hypothesis that size and growth of untreated intracranial meningiomas derived from T1 3D-Gd and

2D-T2WI sequences show good agreement, which would, should this be the case, question the added value of Gd-based contrast media for routine follow-up MRIs of intracranial meningiomas.

## MATERIALS AND METHODS

### Subjects

The Ethics Committee of Geneva University approved this retrospective cohort study. Patient consent was waived. All patients with meningiomas who underwent brain MR imaging with Gd-based contrast media between May 2007 and May 2019 were retrieved from the radiology information system of our institution using the thesaurus feature with the appropriate search terms ("brain MR imaging," "meningioma," "Dotarem"), which searches for exact matches.

The initial search identified 205 patients. Pre-hoc inclusion criteria were adult patients with symptomatic or asymptomatic intracranial meningiomas who had undergone brain MR imaging, including at least T1 3D-Gd and axial 2D-T2WI sequences, in cases in which the radiologic diagnosis

of meningioma was practically certain. Pre-hoc exclusion criteria were uncertain diagnosis of meningioma; meningiomas in the context of a syndrome such as neurofibromatosis type 2, optic nerve, intraosseous, and en plaque meningiomas; and previously treated meningiomas, surgically or otherwise. Eighty-three patients and 256 MR scans were excluded on the basis of these criteria. A total number of 122 patients (35 men, 87 women) was analyzed (Fig 1). The analysis was conducted on the entire cohort as a whole, but a subgroup analysis by meningioma location (skull base versus non-skull base), meningioma size (maximum 3D diameter  $\leq 20$  versus  $> 20$  mm), and symptoms (asymptomatic versus symptomatic) was also performed.

To estimate tumor growth, we included only MRIs in which the time interval between the index scan and subsequent scans was at least 2 years (730 days). Because meningiomas are slow-growing tumors, shorter time periods were excluded to allow detection of tumor growth and to minimize measurement error when calculating annual tumor growth, in which a small error could potentially be multiplied several-fold if a very short time interval was used. Tumor growth was calculated between the index scan and each subsequent scan available for that particular patient. Thirty meningiomas from 26 patients met the time interval criterion of at least 730 days between the index scan and subsequent scans, producing a total of 51 data points. Annual growth for each dimension and geometric parameter was calculated and normalized to annual growth expressed as both the absolute value and percentage change per year to allow comparison.

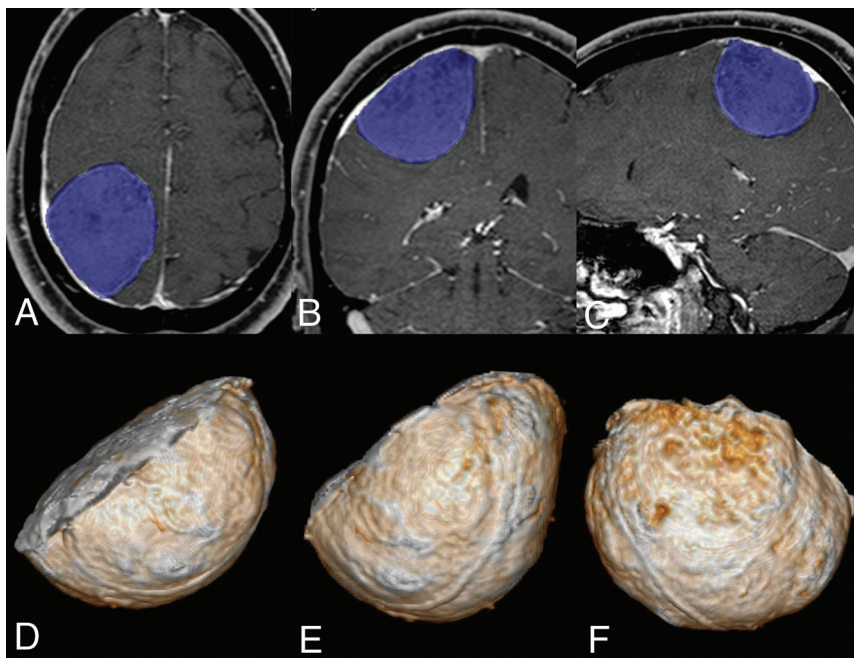


**FIG 2.** A 41-year-old man with a meningioma of the right convexity adjacent to the parietal lobe. Segmentation of the meningioma is achieved by shading the lesion in blue using a semi-automated software (A–C). The voxels outside the shaded volume can be discarded, and the voxels within the volume (shown as 3D-rendering in D, E, and F) can be isolated and exported to the PACS or any other software for further analysis.

The meningioma locations were classified according to studies by Al-Mefty et al<sup>27</sup> and Meling et al,<sup>28</sup> in which cerebral convexity, parasagittal, falcine, intraventricular, and cerebellar convexity meningiomas were considered non-skull base, and all other intracranial locations were considered skull base.

### MR Imaging Protocol

Patients were scanned on 3T and 1.5T Siemens (Siemens Healthcare, Erlangen, Germany), Philips (Philips, Best, The Netherlands), and GE (GE Healthcare, Chicago, Illinois, USA) scanners. As mentioned before, only MR imaging studies that included at least an isotropic, enhanced 3D-T1 sequence (0.6- to 1.1-mm section thickness, no gap between slices) and a conventional axial 2D-T2WI sequence (4-mm section thickness, 0.4-mm gap between slices) were considered. The former was either MPRAGE or a volumetric interpolated breath-hold examination (VIBE; Siemens), 3D-T1 fast-field echo or T1-weighted high-resolution isotropic volume examination (THRIVE; Philips Healthcare), fast 3D gradient echo brain volume imaging (GRE BRAVO; GE Healthcare), or fast acquisition with multiphase elliptic fast gradient-echo (FAME; GE Healthcare). The technical parameters of these sequences can be found in the Online Supplemental Data. Most scans were obtained in our institution; however, a small number of scans included in this study originated from outside institutions. The technical parameters of the sequences from these institutions were roughly similar to those of our center.

### Segmentation and Morphometry

All meningiomas were segmented using a semi-automated software (advanced visualization platform IntelliSpace Portal [ISP],

Version 10.1; Philips Healthcare) on both the T1 3D-Gd and axial T2WI sequences. This method consists of isolating the voxels of the lesion by gradually shading ROIs that automatically grow according to an algorithm based on pixel intensity and proximity. This process can be repeated in all 3 planes until the operator is satisfied that all the voxels of the mass have been selected. The segmentations were performed by J.B. and R.G. (Fig 2), each author having performed approximately half of all the workload. J.B. is a neuro-radiologist with 5 years' experience, and R.G. is a neurosurgeon who received guidance and training before performing the segmentation. In all cases, the quality of the segmentation was overseen by J.B. Shape and volume features were then automatically computed for all meningiomas using Pyradiomics (Version 2.2.0; <https://github.com/AIM-Harvard/pyradiomics>).<sup>29</sup> The following resulting 10 features were thus obtained for all meningiomas and for the segmentations on the T1 3D-Gd and T2WI sequences: tumor volume,

tumor surface area, surface/volume ratio, maximum 3D diameter, maximum 2D diameter in the axial plane, maximum 2D diameter in the coronal plane, maximum 2D diameter in the sagittal plane, major axis length, minor axis length, and least axis length.

### Statistical Analysis

Agreement between the dimensions and geometric parameters obtained from the T1 3D-Gd and T2WI segmentations was assessed by the intraclass correlation coefficient (ICC). Statistical analysis of the data was performed with SPSS Statistics (IBM). A significance level of .05 was used for all statistical tests.

## RESULTS

### Demographics and Descriptive Statistics

The mean patient age at the date of the first available MR imaging scan was 64.7 (SD 17.5) years; range, 22.8–96.0 years). A total of 132 intracranial meningiomas from 122 patients were analyzed. Ninety-three meningiomas (70.5%) were symptomatic, whereas 39 (29.5%) were asymptomatic. Fifty-nine of the 132 meningiomas included underwent surgical resection. Fifty-four of these (91.5%) were WHO grade I, and 5 (8.5%) were grade II. Most patients had a single intracranial meningioma (115/122, 94.3%), 6 patients had 2 meningiomas (4.9%), and 1 patient had 5 meningiomas (0.8%). Two of the 6 patients who had 2 meningiomas on the first MR imaging scan underwent surgical resection of one of the tumors, leaving them with a single lesion on the subsequent follow-up MR imaging. In our cohort, there were 73 non-skull base (55%) and 59 skull base (45%) meningiomas. Distribution of



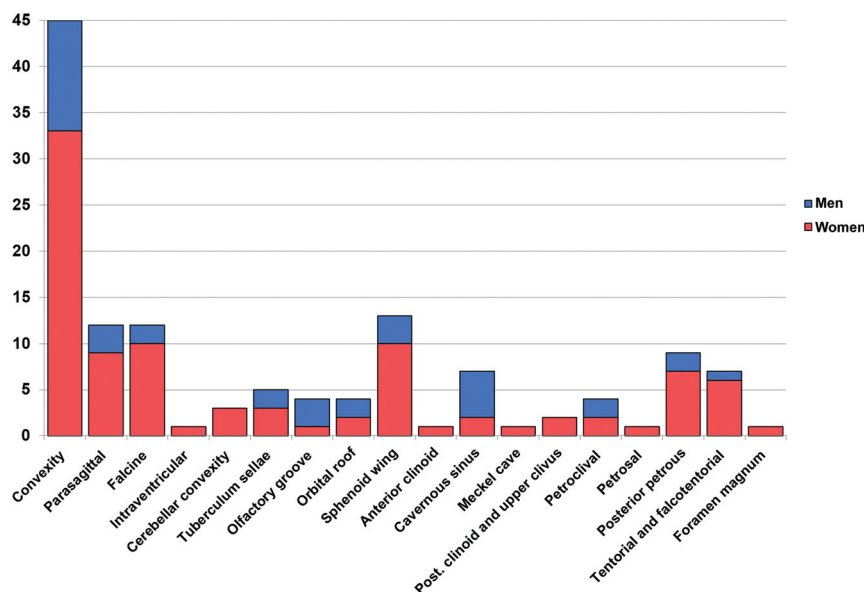


**FIG 3.** Chart showing the number of included intracranial meningiomas by sex and specific location. Cerebral convexity parasagittal, falcine, intraventricular, and cerebellar convexity meningiomas are considered non-skull base. All other locations are considered skull base. Post. indicates posterior.

meningiomas according to sex and specific location are shown in [Fig 3](#) and the Online Supplemental Data.

A total of 259 MR scans were included, 217 (83.8%) from our own center and 42 (16.2%) from outside institutions. A single MR scan was available for 71 of the 132 meningiomas (54%) from 67 of 122 (55%) patients. The remaining 61 meningiomas (46%) from 55 patients were scanned at least twice, enabling analysis of annual tumor growth. Thirty meningiomas (24 from women, 6 from men; 16 non-skull base, 14 skull base) from 26 patients (20 women, 6 men) met the time-interval criterion of at least 730 days between the index scan and subsequent scans, producing a total of 51 data points. The mean time period between scans was 1485 (SD, 864) days (range, 760–3810 days).

### Quantitative Analysis

There was excellent agreement among all parameters derived from the segmentation of meningiomas on the T1 3D-Gd and T2-weighted sequences ( $P < .001$ ): tumor volume (T1 3D-Gd: 9012.15 [SD, 19,223.03] mm<sup>3</sup>; T2WI: 8528.45 [SD, 18,368.18] mm<sup>3</sup>; ICC = 0.996), surface area (ICC = 0.989), surface/volume ratio (ICC = 0.924), maximum 3D diameter (T1 3D-Gd: 26.21 [SD, 15.76] mm, T2WI: 27.49 [SD, 16.02] mm, ICC = 0.986), maximum 2D diameter in the axial plane (ICC = 0.990), maximum 2D diameter in the coronal plane (ICC = 0.982), maximum 2D diameter in the sagittal plane (0.985), major axis length (T1 3D-Gd: 21.92 [SD, 13.16] mm; T2WI: 22.48 [SD, 13.00] mm, ICC = 0.989), minor axis length (ICC = 0.992), least axis length (ICC = 0.988) (Online Supplemental Data). [Figures 4 and 5](#) show examples of T1 3D-Gd- and T2WI-based segmentations of meningiomas in different locations.

The agreement between T1 3D-Gd and T2WI measurements was also excellent in the subgroup analysis of meningiomas according to location, size, and symptoms with ICCs higher than

0.9 in most cases and generally above 0.8 ( $P < .001$ ), including meningiomas with a maximum 3D diameter of  $\leq 20$  mm. Excellent ICCs ( $> 0.9$ ) were found for all subgroups in tumor volume, maximum 3D diameter, and maximum 3D diameter in the axial plane. For example, the ICC for tumor volume for asymptomatic lesions was 0.997 (T1 3D-Gd: 6353.99 [SD, 14,245.73] mm<sup>3</sup>; T2WI: 6022.21 [SD, 14,022.95] mm<sup>3</sup>); and 0.993 for symptomatic meningiomas (T1 3D-Gd: 17,179.23 [SD, 28,322.25] mm<sup>3</sup>; T2WI: 16,228.74 [SD, 26,444.90] mm<sup>3</sup>). As this example shows, this analysis also revealed that symptomatic meningiomas tended to be larger than asymptomatic lesions but also that, despite this difference, the agreement between the 2 different sequences was not meaningfully affected. The results of the subgroup analysis are shown in the Online Supplemental Data.

The data used to assess annual tumor growth showed good-to-excellent agreement (ICC = 0.820–0.989,  $P < .001$ ) between the T1 3D-Gd and T2WI segmentations, expressed both in absolute values and relative change per year when we used the following measurements: tumor volume (T1 3D-Gd: 461.87 [SD, 2704.17] mm<sup>3</sup>/year, 9.24 [SD, 22.55]%/year; T2WI: 556.64 [SD, 2624.02] mm<sup>3</sup>/year, 15.82 [SD, 32.00]%/year), tumor surface area (T1 3D-Gd: 87.03 [SD, 371.66] mm<sup>2</sup>/year, 5.73 [SD, 12.66]%/year; T2WI: 112.01 [SD, 453.59] mm<sup>2</sup>/year, 15.82 [SD, 32.00]%/year), maximum 3D diameter (T1 3D Gd: 0.56 [SD, 1.79] mm/year, 2.38 [SD, 6.12]%/year; T2WI: 0.72 [SD, 1.95] mm/year, 3.16 [SD, 7.02]%/year), and major axis length (T1 3D Gd: 0.51 [SD, 1.57] mm/year, 2.42 [SD, 5.86]%/year; T2WI: 0.67 [SD, 1.64] mm/year, 3.52 [SD, 7.45]%/year). Of note, the T2WI segmentation tended to overestimate tumor-interval growth despite the good agreement with the T1 3D-Gd segmentation. The same analysis performed on other measurements used to evaluate tumor growth (eg, surface/volume ratio, maximum 2D diameter in the axial plane, maximum 2D diameter in the coronal plane, maximum 2D diameter in the sagittal plane, minor axis length, and least axis length) also produced significant results, albeit less striking, with ICCs ranging from 0.631 to 0.901 ( $P < .001$ ). The agreement was generally better when absolute rather relative growth was considered. These results are summarized in the Online Supplemental Data.

### DISCUSSION

In this single-institution, retrospective cohort study of 123 adult patients with symptomatic or asymptomatic intracranial meningiomas with both skull base and non-skull base locations, a total of 282 MR scans were analyzed to assess the value of Gd-based contrast media for routine follow-up MRIs with respect to tumor size and growth.

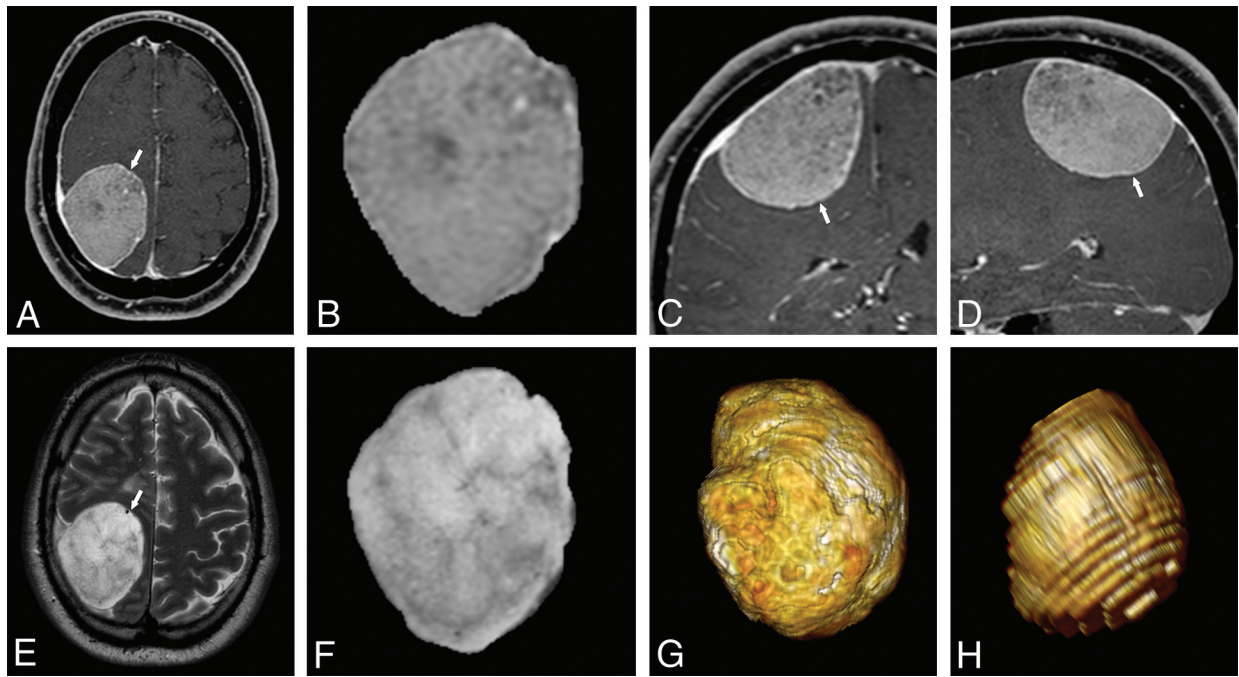


**FIG 4.** Same patient as in Fig 2 with a meningioma of the right convexity adjacent to the parietal lobe. Axial (A), coronal (C) and sagittal (D) THRIVE Gd and axial T2-weighted (E) images depict a meningioma of the right convexity exerting mass effect on the adjacent brain parenchyma of the parietal lobe (arrow, A, C, D, and E). Axial THRIVE Gd (B) and T2-weighted (F) images of the isolated lesion obtained with the semi-automated software, from which 3D-rendering can easily be performed with any DICOM viewer (G, THRIVE Gd. H, T2WI).

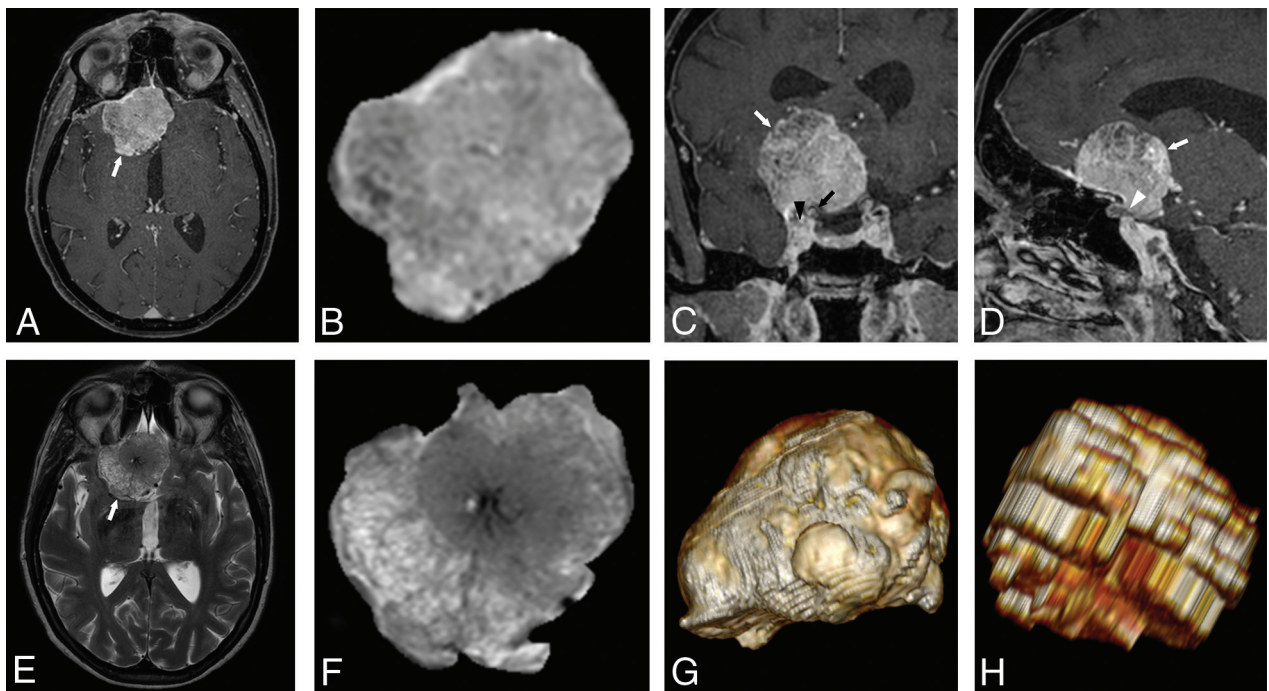


**FIG 5.** A 52-year-old woman. Axial (A), coronal (C) and sagittal (D) THRIVE Gd and axial T2-weighted (E) images show a meningioma arising from the planum sphenoidale and orbital roof on the right (white arrow, A, C, D, and E). The lesion crosses the midline and is in close contact with the cisternal segment of the right optic nerve (white arrowhead in D), the supraclinoid right internal carotid artery (black arrow, C), and cranial aspect of the right cavernous sinus (black arrowhead, C). Axial THRIVE Gd (B) and T2-weighted (F) images of the isolated lesion obtained with the semi-automated software, from which 3D-rendering was performed with our DICOM viewer (G, TI 3D-fat-saturated Gd; H, T2WI). This case illustrates a particularly challenging meningioma for which the skull base location, close contact with other structures, and irregular shape made the segmentation process more difficult.

### **Individual Measures and Tumor Growth**

Our study demonstrates that the absolute agreement among parameters obtained from the T1 3D-Gd and T2WI sequences with respect to tumor volume, maximum 3D diameter, maximum 2D diameters in 3 planes, and major axis length was near-perfect, despite T2WI sequences being 2D with 4-mm section thickness and a 0.4-mm gap between slices, demonstrating the value of such noncontrast sequences for the follow-up of untreated meningiomas. This feature proved to be the case even across a variety of 9 scanner models from 2 different manufacturers in our institution and also a third scanner manufacturer from outside institutions, thus reinforcing the robustness of the agreement we found between T1 3D-Gd and T2WI segmentations.

An important point is the subgroup analysis we performed to investigate whether the agreement between the 2 sequences remained acceptable if only certain types of meningiomas were considered. The agreement between T1 3D Gd and T2 remained adequate for meningiomas in different locations, smaller-versus-larger meningiomas, and also symptomatic-versus-asymptomatic lesions for all the different single-time-point measurements, including the most important ones such as tumor volume, maximum 3D diameter, and maximum diameter in all 3 planes. The subgroup analysis also found that symptomatic meningiomas tended to be larger than asymptomatic lesions, as expected. These high ICC values provide, in our opinion, further reassurance that our method was consistent and that noncontrast MR imaging could potentially suffice for the follow-up of a wide variety of meningiomas, including symptomatic lesions. We understand, however, that the case could be made for the use of Gd contrast media for a small proportion of aggressive and infiltrative meningiomas in very specific locations, which could hinder an appropriate imaging work-up, at least in the first scan.

The growth rate of intracranial meningiomas is one of the most important factors influencing the decision for surgical treatment, with immediate intervention at diagnosis having the potential for unnecessary treatment.<sup>30</sup> Furthermore, because most asymptomatic meningiomas do not exhibit growth, the best management option may be conservative treatment with imaging follow-up, thus avoiding surgery-related morbidity.<sup>25</sup> Serial imaging allowed us to evaluate tumor growth. A conscious decision was made to include only meningiomas in which the follow-up was at least 2 years, to minimize errors as much as possible. Absolute tumor growth (evaluated as an annual increase in tumor volume, tumor surface area, maximum 3D diameter, and major axis length) obtained from the T1 3D-Gd and T2WI segmentations showed excellent agreement between the 2 sequences with near-perfect ICCs. The agreement for relative annual tumor growth expressed as %/year was slightly lower, probably reflecting that more computation was needed to obtain relative annual growth, but it was still very high with  $P < .001$  in all cases. Because MR imaging follow-up of intracranial meningiomas is primarily performed to assess tumor growth, our results are both encouraging and reassuring, indicating that Gd-based contrast might not add enough value and could potentially be omitted.

An important point is that contrast medium is usually administered in follow-up MR imaging of intracranial meningiomas because it is thought to allow improved delineation of invasion of

the dural venous sinuses by a lesion, such as the sagittal, straight, or cavernous sinuses. Nevertheless, we found that visualization of vascular invasion by meningiomas is often hindered on T1 Gd-weighted sequences, in which enhancement of the meningioma is sometimes difficult to distinguish from opacification of the venous sinus itself, and that vascular invasion is often better depicted on T2WI as an absence of flow void and by direct visualization of the edges of the meningioma itself. This is the case with gradient-echo T1 3D-Gd sequences, which are routinely performed as part of the meningioma follow-up imaging protocol at our institution. While it is true that black-blood Cube (GE Healthcare) or sampling perfection with application-optimized contrasts by using different flip angle evolution (SPACE; Siemens) sequences would mitigate this limitation, they would also depict other anatomic structures in less detail, especially near the skull base, including the meningioma itself and brain tissue. Image-acquisition time would also be prolonged with this type of sequence. Another important point in this respect is that while it is true that the absence of flow voids on T2WI does not always reflect sinus invasion by the meningioma, dural sinus invasion could be evaluated with other noncontrast sequences. Because meningiomas are usually hyperintense on diffusion-weighted imaging due to their high cellularity, this sequence could be used to distinguish slow flow from sinus invasion.

Because one of the advantages of not using contrast media is to reduce imaging time, it seems somewhat counterproductive to include sequences that would increase the image-acquisition time for little gain in quality. At our institution, the actual gain in imaging time if no contrast was used amounts to the time it takes to perform 2D-T1 spin-echo Gd and T1 3D-Gd sequences, which is approximately 8 minutes depending on the scanner. The time savings would be even more striking if we obviated the need for contrast MRV, a sequence usually included in the imaging protocol of meningiomas that invade or compress the dural venous sinuses. However, 3D-T2 sequences can sometimes depict the venous sinuses and structures near the skull base in less detail due to artifacts. In view of these limitations, a sensible compromise could be to keep 2D-T2WI in the imaging protocol and replace the 2D-FLAIR with a 3D-FLAIR sequence.

As mentioned before, health care cost is also an important factor in modern medical practice, not only to patients in private or semi-private health care systems but also to societies. In our center, the direct cost-saving of performing a noncontrast as opposed to a contrast brain MR imaging would be approximately \$500. Indirectly, savings would be even more significant if the reduced image-acquisition time is taken into account. Last and despite the relative safety of Gd contrast media, the short-term and long-term consequences of the administration of contrast media could be avoided and patient safety could be improved.

### **Literature**

The excellent agreement between absolute annual tumor growth obtained from the T1 3D-Gd and T2WI segmentations strongly suggests that noncontrast MR imaging is adequate for the follow-up of most intracranial meningiomas. Our results are in agreement with those by He et al,<sup>31</sup> in 2020, who assessed the suitability of T2WI sequences for long-term follow-up of asymptomatic



convexity meningiomas. However, our study differs from this one in several points, specifically a larger number of patients (123 versus 18), also including skull base meningiomas as well as both symptomatic and asymptomatic meningiomas, and our study tumor size being assessed by a semi-automated method, thus minimizing interoperator error.

The behavior of skull base meningiomas is different from that of non-skull base meningiomas, and skull base meningiomas have shorter retreatment-free survival.<sup>28</sup> Notwithstanding some difficulties we encountered with the segmentation of skull base meningiomas in certain locations (in the cavernous sinus and near the orbits), we were reasonably confident that our method had adequate accuracy for all intracranial locations, and we also included skull base meningiomas in our study, which are known to behave differently and exhibit faster growth rates than non-skull base meningiomas as observed by Hashimoto et al,<sup>32</sup> in 2012. The fact that the agreement between the two different sequences remained acceptable for skull base meningiomas provided some validation to the decision of including these meningiomas in our study.

### Strengths and Limitations

We believe that one of the strengths of our study is that an accurate semi-automated segmentation method was considered from the early planning stages of this study to minimize subjectivity and operator-related variability as much as possible. Furthermore, we included parameters that are not generally used in routine clinical practice such as the least axis length and minor axis length of the tumor, to further confirm the accuracy of the segmentation and the measurements. Another strong point, in our opinion, is that we did not exclude skull base or symptomatic meningiomas, making our results more generalizable and holding higher external validity than if we had focused only on convexity meningiomas.

The main limitations of this study are its retrospective rather than prospective nature and also the potential bias that was introduced by the segmentation process, which was not blinded between the T1 3D-Gd and T2-weighted images, as each meningioma was segmented by the same operator. The decision to perform the segmentation in this manner was made at the beginning of the study in order to allow the considerable workload to be shared and to expedite the segmentation process. Another limitation is that although some MR imaging studies from external institutions were included, it remains a single-center study. Other limitations relate to the technical aspects of the semi-automated segmentation; we found that delineation of skull base meningiomas in certain locations posed considerable difficulties due to adjacent anatomic structures with similar signal intensities. Although care was taken to perform the segmentation of these meningiomas as thoroughly as possible, we acknowledge that some inaccuracies may have occurred while performing the segmentation of meningiomas of the cavernous sinus, both on T1 3D-Gd and T2WI, and those near the orbits on T2WI. A case of a meningioma for which the segmentation was particularly challenging is illustrated in Fig 5. T2WI-based segmentation tended to overestimate tumor growth. This feature was probably due to the effects of partial volume averaging, which are to be expected when a 2D sequence is used to generate 3D parameters, particularly on lesions that are irregularly shaped. We believe this overestimation could,

however, be easily overcome if a 3D volumetric T2-weighted sequence was used, which could be a topic of future research.

### CONCLUSIONS

Our results show excellent agreement between dimension and geometric parameters of meningiomas derived from T1 3D-Gd and T2-weighted sequences, suggesting that the use of Gd-based contrast agents in follow-up MR imaging of untreated meningiomas should be carefully reviewed because the use of gadolinium might not offer enough added value for assessing tumor size and growth rates. Furthermore, noncontrast MR imaging would avert risks associated with contrast media, be more cost effective, and reduce image-acquisition time.

### REFERENCES

1. Prince MR, Zhang H, Zou Z, et al. **Incidence of immediate gadolinium contrast media reactions.** *AJR Am J Roentgenol* 2011;196:W138–43 [CrossRef Medline](#)
2. Granata V, Cascella M, Fusco R, et al. **Immediate adverse reactions to gadolinium-based MR contrast media: a retrospective analysis on 10,608 examinations.** *BioMed Res Int* 2016;2016:3918292 [CrossRef Medline](#)
3. Kanda T, Ishii K, Kawaguchi H, et al. **High signal intensity in the dentate nucleus and globus pallidus on unenhanced T1-weighted MR images: relationship with increasing cumulative dose of a gadolinium-based contrast material.** *Radiology* 2014;270:834–41 [CrossRef Medline](#)
4. Kanda T, Osawa M, Oba H, et al. **High signal intensity in dentate nucleus on unenhanced T1-weighted MR images: association with linear versus macrocyclic gadolinium chelate administration.** *Radiology* 2015;275:803–09 [CrossRef Medline](#)
5. Quattrocchi CC, Mallio CA, Errante Y, et al. **Gadodiamide and dentate nucleus T1 hyperintensity in patients with meningioma evaluated by multiple follow-up contrast-enhanced magnetic resonance examinations with no systemic interval therapy.** *Invest Radiol* 2015;50:470–72 [CrossRef Medline](#)
6. Ramalho J, Semelka RC, Ramalho M, et al. **Gadolinium-based contrast agent accumulation and toxicity: an update.** *AJNR Am J Neuroradiol* 2016;37:1192–98 [CrossRef Medline](#)
7. Stojanov D, Aracki-Trenkic A, Benedeto-Stojanov D. **Gadolinium deposition within the dentate nucleus and globus pallidus after repeated administrations of gadolinium-based contrast agents—current status.** *Neuroradiology* 2016;58:433–41 [CrossRef Medline](#)
8. Huber M, Orosz E. **Health expenditure trends in OECD countries.** *Health Care Financ Rev* 2003;25:1–22 [Medline](#)
9. Reinhardt UE, Hussey PS, Anderson GF. **U.S. health care spending in an international context.** *Health Aff (Millwood)* 2004;23:10–25 [CrossRef Medline](#)
10. Dunnick NR, Applegate KE, Arenson RL. **The inappropriate use of imaging studies: a report of the 2004 Intersociety Conference.** *J Am Coll Radiology* 2005;2:401–06 [CrossRef Medline](#)
11. Goldbrunner R, Minniti G, Preusser M, et al. **EANO guidelines for the diagnosis and treatment of meningiomas.** *Lancet Oncol* 2016;17:e383–91 [CrossRef Medline](#)
12. Buetow MP, Buetow PC, Smirniotopoulos JG. **Typical, atypical, and misleading features in meningioma.** *Radiographics* 1991;11:1087–106 [CrossRef Medline](#)
13. Russell EJ, George AE, Kricheff II, et al. **Atypical computed tomography features of intracranial meningioma: radiological-pathological correlation in a series of 131 consecutive cases.** *Radiology* 1980;135:673–82 [CrossRef Medline](#)
14. Ostrom QT, Gittleman H, Fulop J, et al. **CBTRUS Statistical Report: Primary Brain and Central Nervous System Tumors Diagnosed in**



- the United States in 2012-2016. *Neuro Oncol* 2019;21(Suppl 5):v1-100 [CrossRef Medline](#)
15. Wood MW, White RJ, Kernohan JW. One hundred intracranial meningiomas found incidentally at necropsy. *J Neuropathol Exp Neurol* 1957;16:337-40 [CrossRef Medline](#)
  16. Nakamura M, Roser F, Michel J, et al. Volumetric analysis of the growth rate of incompletely resected intracranial meningiomas. *Zentralbl Neurochir* 2005;66:17-23 [CrossRef Medline](#)
  17. Lee EJ, Kim JH, Park ES, et al. A novel weighted scoring system for estimating the risk of rapid growth in untreated intracranial meningiomas. *J Neurosurg* 2017;127:971-80 [CrossRef Medline](#)
  18. Nakasu S, Nakasu Y. Natural history of meningiomas: review with meta-analyses. *Neurol Med Chir (Tokyo)* 2020;60:109-20 [CrossRef Medline](#)
  19. Niiro M, Yatsushiro K, Nakamura K, et al. Natural history of elderly patients with asymptomatic meningiomas. *J Neurol Neurosurg Psychiatry* 2000;68:25-28 [CrossRef Medline](#)
  20. Nakamura M, Roser F, Michel J, et al. The natural history of incidental meningiomas. *Neurosurgery* 2003;53:62-70; discussion 70-71 [CrossRef Medline](#)
  21. Hashiba T, Hashimoto N, Izumoto S, et al. Serial volumetric assessment of the natural history and growth pattern of incidentally discovered meningiomas. *J Neurosurg* 2009;110:675-84 [CrossRef Medline](#)
  22. Oya S, Kim SH, Sade B, et al. The natural history of intracranial meningiomas. *J Neurosurg* 2011;114:1250-56 [CrossRef](#)
  23. Jadid KD, Feychting M, Höijer J, et al. Long-term follow-up of incidentally discovered meningiomas. *Acta Neurochir (Wien)* 2015;157:225-30 [CrossRef Medline](#)
  24. Romani R, Ryan G, Benner C, et al. Non-operative meningiomas: long-term follow-up of 136 patients. *Acta Neurochir (Wien)* 2018;160:1547-53 [CrossRef Medline](#)
  25. Yano S, Kuratsu JI. Kumamoto Brain Tumor Research Group. Indications for surgery in patients with asymptomatic meningiomas based on an extensive experience. *J Neurosurg* 2006;105:538-43 [CrossRef Medline](#)
  26. Sughrue ME, Rutkowski MJ, Aranda D, et al. Treatment decision making based on the published natural history and growth rate of small meningiomas. *J Neurosurg* 2010;113:1036-42 [CrossRef Medline](#)
  27. Al-Mefty O, McDermott MW, DeMonte F. *Al-Mefty's Meningiomas*. 2nd ed. Thieme Medical; 2011
  28. Meling TR, Da Broi M, Scheie D, et al. Meningiomas: skull base versus non-skull base. *Neurosurg Rev* 2019;42:163-73 [CrossRef Medline](#)
  29. van Griethuysen JJ, Fedorov A, Parmar C, et al. Computational radiomics system to decode the radiographic phenotype. *Cancer Res* 2017;77:e104-07 [CrossRef Medline](#)
  30. Islim AI, Mohan M, Moon RDC, et al. Incidental intracranial meningiomas: a systematic review and meta-analysis of prognostic factors and outcomes. *J Neurooncol* 2019;142:211-21 [CrossRef Medline](#)
  31. He JQ, Iv M, Li G, et al. Noncontrast T2-weighted magnetic resonance imaging sequences for long-term monitoring of asymptomatic convexity meningiomas. *World Neurosurg* 2020;135:e100-05 [CrossRef Medline](#)
  32. Hashimoto N, Rabo CS, Okita Y, et al. Slower growth of skull base meningiomas compared with non-skull base meningiomas based on volumetric and biological studies. *J Neurosurg* 2012;116:574-80 [CrossRef Medline](#)